

÷

## 

E. W. Castner, Jr. and Y. J. Chang

Femtosecond Dynamics in **Hydrogen-Bonded Solvents** 

solvent relaxation dynamics. In turn, specific features of the solvent relax-LECEIV ation dynamics in molecular liquids SEP 0 3 1995 ave long been studied by techniques such as magnetic resonance T<sub>1</sub>-relax-OSTIation, dielectric relaxation, Rayleigh and Raman light-scattering, and far-infrared absorption spectroscopy, in addition to the more recent ultrafast laser techniques, such as the time-dependent fluorescence Stokes-shift (TDFSS).

> We present results using a femtosecond laser polarization spectroscopy technique that encompass all of the ultrafast dynamical results of the above mentioned experiments. Our ultrafast laser spectroscopy data provide a holistic solvent relaxation profile that includes the longer-time diffusive solvent relaxation dynamics, in addition to the more rapid inertial motions. The inertial motions include librations, translations, and collisions. By obtaining a complete profile of the neat solvent dynamics on all relevant timescales, we can then test theoretical predictions and molecular dynamics simulations that model the effect of solvent relaxation on the solvation dynamics. These solvent dynamics can directly affect the outcome of chemical reactions. In this contribution, we present the results of our recent experiments on the femtosecond relaxation of the dipolar, strongly associated, and hydrogen-bonding liquids formamide, Nmethylformamide (NMF), dimethylformamide (DMF), acetic acid, water, and ethylene glycol.

The time-resolved optical Kerr effect has been used to study molecular liquids since Duguay and Hansen generated an optical gate in CS2 (Duguay and Hansen, 1969). In the past decade, several workers have used a heterodyne scheme (Levenson and Eesley, 1979) to make the detected

### ABSTRACT

We present results on the ultrafast dynamics of pure hydrogen-bonding solvents, obtained using femtosecond Fourier-transform optical-heterodynedetected, Raman-induced Kerr effect spectroscopy. Solvent systems we have studied include the formamides, water, ethylene glycol, and acetic acid. Inertial and diffusive motions are clearly resolved. We comment on the effect that such ultrafast solvent motions have on chemical reactions in solution.

### INTRODUCTION

Many solution-phase chemical transformations have a strong dependence on both the static and dynamic properties of the solvent. When considered in greater detail, macroscopic properties of solvents such as viscosity or dielectric constant are actually a measure of the microscopic structure and dynamics of molecular liquids. One class of solution-phase reactions for which the solvation-coordinate is strongly coupled to the reaction coordinate is that of adiabatic charge-transfer reactions. In particular, certain electron-transfer reactions in the barrierless regime have effective rates that are predicted to be limited by the

MASTER de

### **DISCLAIMER**

This report was prepared as an account of work sponsored by an agency of the United States Government. Neither the United States Government nor any agency thereof, nor any of their employees, makes any warranty, express or implied, or assumes any legal liability or responsibility for the accuracy, completeness, or usefulness of any information, apparatus, product, or process disclosed, or represents that its use would not infringe privately owned rights. Reference herein to any specific commercial product, process, or service by trade name, trademark, manufacturer, or otherwise does not necessarily constitute or imply its endorsement, recommendation, or favoring by the United States Government or any agency thereof. The views and opinions of authors expressed herein do not necessarily state or reflect those of the United States Government or any agency thereof.

signal linear in the molecular nonlinear optical response (Greene and Farrow, 1982; McMorrow, et al., 1988; McMorrow, 1991; McMorrow and Lotshaw, 1991; Cho, et al., 1992; McMorrow, et al., 1992; Wynne, et al., 1992; Chang and Castner, 1993; McMorrow and Lotshaw, 1993). Optical-heterodyne detected, Ramaninduced Kerr-effect spectroscopy (OHD-RIKES) is a very sensitive nonlinear optical technique that measures the time-dependent relaxation of a coherent macroscopic polarization induced in the transparent liquid sample by an intense femtosecond pulse with a peak power-density of ≤2 GW/cm<sup>2</sup>, and probed by a probe pulse about 20 times weaker. As the molecules of the neat liquid sample relax both individually and collectively, they rotate, librate, vibrate, translate, and collide. The coherent macroscopic polarization oscillates and decays as a result of the molecular motions. While the technique is electronically non-resonant, i.e., the samples do not absorb the near-infrared or visible pulses used, the low-frequency intermolecular vibrations are impulsively excited. Using laser pulses of ≤50 femtoseconds, all of the single-molecule and collective motions can be impulsively excited by the broad. Fourier-transform limited spectrum of the actinic pulse. As in the solid state, the low-frequency collective vibrations are expected to couple most strongly with excited states or transition states of reacting species. Hattori, et al. (Hattori, et al., 1991) have developed an analogous technique that also yields the same molecular information.

The impulsive-stimulated-Ramanscattering (ISRS) technique (Ruhman, et al., 1988; Yan, et al., 1988) measures the same ultrafast solvent dynamical properties as our OHD-RIKES experiment, because in both cases, the signal arises from the same molecular nonlinear optical (polarizability) response. When performed in a polarization-sensitive transient-grating/fourwave-mixing folder BOXCARS geometry, the ISRS experiment has the distinct advantage of being able to measure either pure nuclear-coordinate or pure electronic dynamics directly (Etchepare, et al., 1987). In this case, suppression of the electronic hyperpolarizability is clearly advantageous for the study of liquids such as water and ethylene glycol, where the electronic contribution to the molecular nonlinear optical response dominates the signal. There are two drawbacks of ISRS relative to OHD-RIKES. They are: i) ISRS requires pulse-energies in the range of 100 nJ-1 µJ, while OHD-RIKES pulse energies need only be in the 100 pJ-5 nJ range, and ii) the ISRS signal is proportional to the square of the molecular nonlinear optical response, while OHD-RIKES signals are linear in the same response. Point i) is not a limitation in many laboratories. where femtosecond pulse energies after amplification of a pico-/nano-Joule oscillator to up to >1 mJ is now a standard technology. However, it is quite convenient to be able to do the OHD-RIKES experiment with an un-amplified Ti:Sapphire femtosecond oscillator. With regard to point ii): the square of the molecular response will contain cross-terms that complicate the analysis of ISRS data relative to OHD-RIKES data, without adding any additional molecular dynamical information. On the other hand, strain-birefringence is a difficult problem in extending the OHD-RIKES experiment to extremes of low-temperatures (in cryostats) and high-pressures (in diamond-anvil cells). These limitations have been overcome for the study of the femtosecond dynamics of CS2 using the ISRS technique (Ruhman, et al., 1987; Kohler and Nelson, 1992). Thus, because each technique has clear merits and disadvantages, the ideal will be to select one or the other based on the limitations imposed by the liquid under study, such as the magnitude of the total molecular nonlinear optical response, and the relative amplitudes of the electronic versus the nuclear contributions to this response.

A general feature of our femtosecond solvent dynamical results is that in all liquids there appears a clear separation of time-scales between diffusive and inertial dynamics. The diffusive dynamics are temperature-dependent, while the inertial (or non-diffusive) dynamics are only weakly temperature dependent. Previous studies of solvent dynamics by dielectric relaxation, NMR T<sub>1</sub> relaxation, and Rayleigh light scattering have tended to concentrate on the diffusive component of the dynamics, which leads to predictions for solvent-dependent chemical reaction rates that are too slow. Rayleigh and Raman spectroscopy signals arise from the same molecular polarizability tensor that is responsible for the OHD-RIKES signal, but because of our timedomain measurement, we can easily separate the diffusive (Lorentzian) and inertial parts of the low-frequency dynamics. By combining data analysis in the time and frequency domains, which is possible because we use Fouriertransform limited laser pulses, we can develop appropriate models that take into account lineshapes, dephasing rates, lifetimes, and relative amplitudes of the different motions contributing to the ultrafast solvent relaxation.

### **EXPERIMENTAL**

The experimental setup we use to measure femtosecond solvent dynamics by the OHD-RIKES experiment has been described in detail recently by several authors (McMorrow, Lotshaw et al. 1988; McMorrow and Lotshaw 1991; Chang and Castner 1993; Chang and Castner 1993.). Thus only a few brief comments will be given here. One important feature of our experiment is that we are using an ultra-stable modelocked Ti:Sapphire laser for our source of femtosecond pulses. We routinely use pulses of ~50 fs, with a sech<sup>2</sup> pulse shape. Spectra-Physics Tsunami laser gives an output at 780 nm of ~650 mW at 82 MHz repetition rate, or ~8 nJ/pulse, when pumped by 6.0 W from an alllines BeamLok 2060-7S Ar+ laser in a TEM<sub>00</sub> spatial mode.

A schematic diagram of the experimental setup is shown in Figure 1. The geometry is that of a standard pumpprobe polarization experiment, where an uncoated wedge splits off ~5% of the beam for the probe, with the remainder used for the pump. A Glan-Laser calcite polarizer sets the vertical polarization of the pump beam, while the probe beam is rotated to +45° for a maximal projection of the probe onto both axes of the induced birefringence. Glan-Thompson calcite polarizers are used in the probe beam, with a mica quarter-wave retarder located before the sample. When all optics in the probe beam are set for maximum extinction, the ratio of probe transmitted through blocked and fully open polarizers has been measured to be 1.6x10-8. including the sample cell, sample, and focusing lenses. The calcite polarizers are obtained from Karl Lambrecht Corp., and the mica waveplates from Optics for Research. The zero-order half-wave retarders were from Newport Corp., and the 1 mm path fused silica sample cells were from NSG Precision Cells.

An out-of-phase local-oscillator is generated for the optical-heterodyne

detection by rotating the input polarizer by 1°. The out-of-phase local-oscillator heterodyne signal is measured to be a factor of 30-50 times greater than the homodyne signal obtained when the

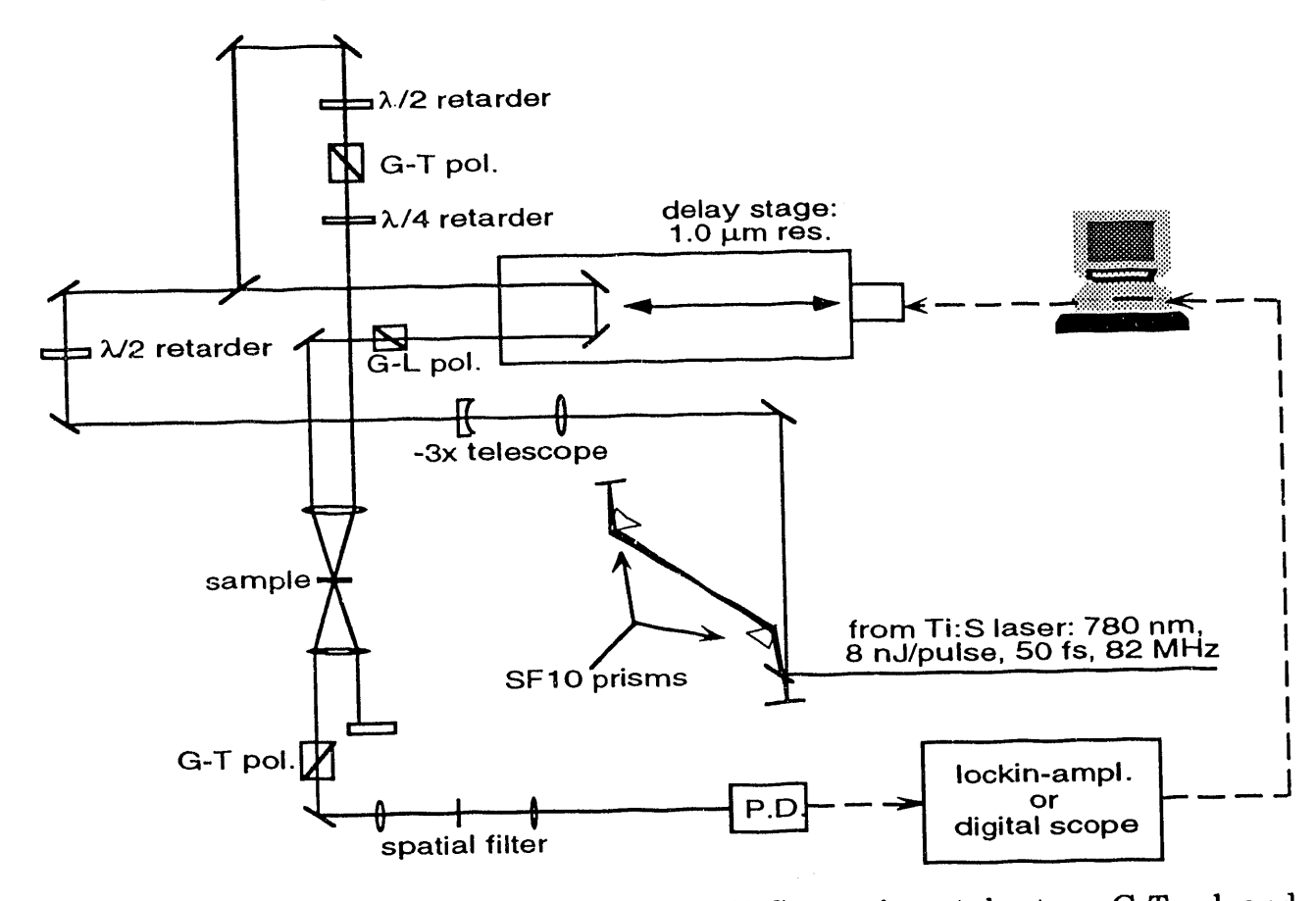


Figure 1. Schematic diagram for the OHD-RIKES experimental setup. G-T pol. and G-L pol. represent Glan-Thompson and Glan-Laser calcite polarizers, respectively. The pinhole in the spatial filter is  $100\,\mu m$  diameter. P.D. represents the photodetector, either a Hamamatsu R928 photomultiplier or a Thorlabs PDA50 photodiode. The near-retroreflecting SF10 prism pair is a phase compensator for correcting for the group-velocity-dispersion mismatch arising from the normal dispersion of the polarizers and other optics.

polarizers are crossed. The pump beam is scanned with 1.0 µm precision using an Aerotech DC-servo motor stage under real-time computer control via a nuLogic, Inc. interface. Either a Hamamatsu R928 photomultiplier tube or a Thorlabs PDA50 photodiode is used to detect the heterodyned probe beam. Data is acquired either by using the stage as a stepper system, or by rapidly scanning it (3 cm/sec) and acquiring the data on a digital oscilloscope (5  $\mu$ s = 1 femtosecond delay). In either case, a number of scans ranging from 10 to 1000 are averaged either on a computer reading a lockin-amplifier

(stepper case) or on the digital scope (fast scan case). Water has the smallest nonlinear optical response of the liquids we have studied thus far, yet a signal-to-noise ratio of 1000 relative to the peak of the signal was obtained by averaging 10 scans for a room-temperature water sample. A far superior signal-to-noise is of course obtained for liquids with a large nonlinear optical response, such as CS2. Such a high signal-to-noise ratio is required to be able to make best use of the data in later analysis, such as when the electronic response is deconvoluted and the pure nuclear-coordinate motions are considered in the frequency domain.

All solvents were reagent, spectrophotometric, or HPLC grade, and were purified by fractional vacuum distillation immediately prior to use, with the exception of the freshly-opened acetic acid, which was Baker Ultrex grade. Water was obtained from a MilliPore Milli-Q purification system.

## THEORETICAL BACKGROUND

In the OHD-RIKES experiment, an intense femtosecond pump pulse interacts with the liquid sample non-resonantly with respect to electronic states, inducing a macroscopic polarization arising from a coupling between the electric field and the nonlinear optical response, R(t). The signal is detected as a birefringence transient. Because the Born-Oppenheimer approximation applies, the nonlinear optical response R(t) is separable into electronic and nuclear components. These components include an effectively instantaneous electronic hyper-polarizability response,  $\sigma(t)$ , and a slower response limited by the nuclear motions of the sample,  $r_i(t)$ . R(t) is written as:

$$R(t) = \sigma(t) + \sum_{i} r_{i}(t). \qquad (1)$$

While our 50 fs pulses are short, they are certainly not instantaneous. Thus, the birefringence transient that we observe,  $T(\tau)$ , is the convolution of the molecular nonlinear optical response R(t) with the laser pulse autocorrelation,  $G_0^{(2)}(t)$ .  $T(\tau)$  is given by:

$$T(\tau) \propto \int dt \ R(t-\tau) \ G_0^{(2)}(t)$$
 . (2)

To obtain the desired solvent relaxation information contained in the nuclear coordinate part of the response R(t), we must deconvolute the effects of the non-zero impulse width. McMorrow has shown (McMorrow, 1991) that a frequency-domain representation of our data is a means to a straightforward and exact deconvolution method. The frequency-domain susceptibility is defined by

$$D(\omega) = \int_{-\infty}^{\infty} dt \cdot \exp(i\omega t) \cdot R(t) = \mathcal{F}\{R(t)\},$$
(3)

where  $\mathcal{F}$  denotes a forward complex Fourier-transform. We may now write the deconvolution relation as

$$D(\omega) = \frac{\mathcal{F}\{T(\tau)\}}{\mathcal{F}\{G_{\theta}^{(2)}(\tau)\}}.$$
 (4)

 $D(\omega)$  now contains the low-frequency spectral-density free from effects of the non-zero pulse width. For all of the solvents we have studied, our 780 nm laser pulse is electronically non-resonant. The electronic hyperpolarizability component of the nonlinear optical response,  $\sigma(t)$ , is then symmetric and real (following the temporal profile of the autocorrelation of the femtosecond optical pulse). Thus, we can eliminate the electronic hyperpolarizability component from our spectral density by

considering only the imaginary part of  $D(\omega)$ . We define

$$D_{\text{nucl}}(\omega) = \text{Im}[D(\omega)] \tag{5}$$

as the pure nuclear-coordinate frequency-domain representation of our solvent dynamics. We proceed to analyze the low-frequency spectral density in the frequency domain, as well as in the time domain. Time domain analysis of the dynamics can of course be obtained by convolute-and-compare nonlinear least-squares fitting. However, it is convenient to construct the pure nuclear-coordinate component of the nonlinear optical response  $r(t) = \sum_i r_i(t)$  from the inverse Fourier-transform by

$$r(t) = 2\mathcal{F}^{-1} \{ Im[D(\omega)] \} H(t - t_0)$$
 (6)

where H(t) is the Heaviside step-function. The latter technique has the advantage of being model-independent.

A major advantage of femtosecond nonlinear optical spectroscopy, such as OHD-RIKES, over conventional Rayleigh light scattering is that there is a clear and obvious separation of time-scales between diffusive rotational reorientation and faster inertial. non-diffusive dynamics. The longest time-scales in the OHD-RIKES experiment correspond to diffusive relaxation, and can in fact be subtracted away to allow for simpler and more accurate modeling of the inertial parts of the spectral density. The model used for fitting the diffusive relaxation is given in the following equation:

$$r_1(t) = A_{rot} \sum_i c_i \exp(-t/\tau_{ir}) \times [1-\exp(-2\omega_0 t)], \qquad (7)$$

where the  $\tau_{ir}$  are the lifetimes for rotational diffusion, the  $c_i$  are the relative

weights between the lifetimes, A<sub>rot</sub> is the overall amplitude of rotational diffusion in the nuclear-coordinate response, and  $\omega_0$  is the first moment of the intermolecular vibrational band. For the hydrogen-bonding solvents we have studied, at least two exponential components, sometimes three or more, were required to properly fit the longtime tail of the OHD-RIKES birefringence transient data. This multi-exponential character of the solvent rotational diffusion is a manifestation of the fact that these solvent molecules are in general asymmetric rotors with substantially different inertial moments about the different molecular axes.

To make the connection between the pure solvent relaxation data measured in our OHD-RIKES experiments and the solvation coordinate for a charge-transfer reaction, we have implemented an ansatz based upon the recent theory of Maroncelli, et al. (Maroncelli, et al., 1993). Maroncelli model yields a correlation function C<sub>V</sub>(t) for the response of a solvent to an instantaneously created charge.  $C_{V}(t)$  is based on the singlemolecule rotational correlation function taken to the power of the normalized dipole density  $\alpha_{MKP}$ . Our approximation to Cy(t), based on our pure nuclear-coordinate solvent dynamical response, r(t), is (Chang and Castner, 1993):

$$C_{v}(t) \approx \left\{ 1 - \frac{\int_{\mathbf{B}}^{t} r(t')dt'}{\int_{\mathbf{B}}^{\infty} r(t')dt'} \right\}^{\alpha_{MKP}/3}$$
(8)

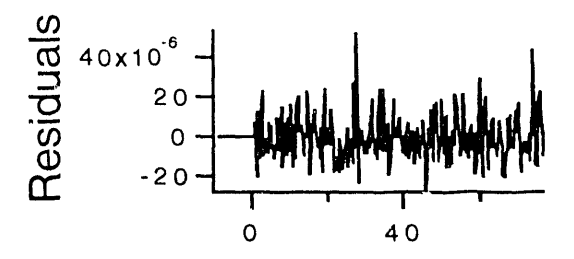
Though a microscopic model including all interactions between the many solvent molecules and the reactant should smooth out much of the oscillatory character of the coherent, inertial solvent response, we find that a rapid femtosecond response occurs in our constructed  $C_V(t)$  functions with a Gaussian shape in the first hundreds of femtoseconds, with a non-exponential component to the solvation relaxation occurring on time scales correlated with the diffusive solvent relaxation.

### RESULTS AND DISCUSSION

On the longest time scales of our OHD-RIKES experiment, ranging from 1-150 picoseconds, only diffusive molecular rotation is occurring in the hydrogenbonding liquids. In all cases, this rotational diffusion correlation cannot be modeled by an exponential decay. Two, three, or more time constants are required. Figure 2 shows the longer timescale rotational diffusion relaxation for acetic acid at 296 K. An excellent fit is obtained for acetic acid when three exponential time constants are used, of lifetimes 0.67, 3.34, and 22.1 ps, respectively. The quality of the fit may be judged by the residuals from the nonlinear least-squares fit; systematic deviations occur when only one or two exponential time constants are used. A quite similar effect is shown to occur for formamides over a range of concentrations in other polar solvents (Chang and Castner, 1993) and over a range of temperatures between 290-360 K. Water and ethylene glycol require two exponential components, with the longer lifetimes for the two solvents being 1.2 and 9.4 ps, respectively.

The shorter time-scale dynamics of the hydrogen-bonding liquids studied are shown in Figures 3 and 4. The raw data are presented in semi-log form, and the frequency-domain representation of the dynamics are shown after deconvolution of the electronic hyperpolarizability response, done using Equations 4 and 5.

All of the OHD-RIKES data sets have a sharply rising leading edge that initially follows the laser-pulse autocorrelation signal. This pulse-response shaped signal component arises from the electronic hyperpolarizability part



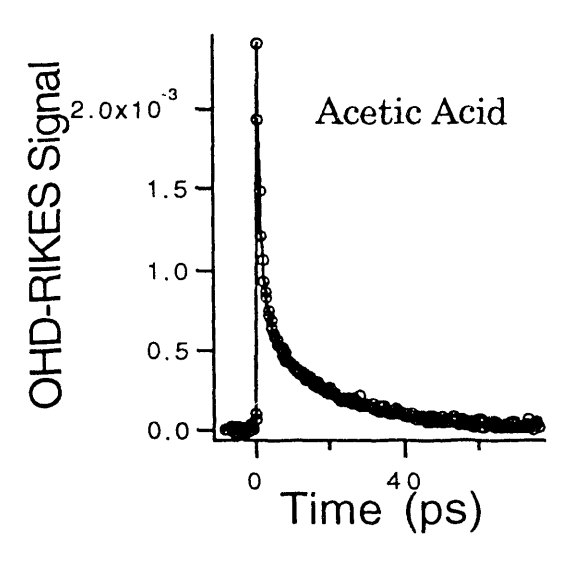


Figure 2. The longer time-scale diffusive rotational reorientation decay is shown for acetic acid at 296 K. The data near zero-time-delay are off-scale. The open circles are the data, and the solid line is the nonlinear least squares fit. The residuals from the fit are shown at the top of the figure. Three exponential time constants are required to fit the data in the range from 1-80 ps. The relative amplitudes and lifetimes are:

 $c_1 = 2.958 \times 10^{-3} \pm 3.4 \times 10^{-4}$ ,  $c_2 = 5.593 \times 10^{-4} \pm 6.9 \times 10^{-5}$ ,  $c_3 = 5.775 \times 10^{-4} \pm 1.3 \times 10^{-5}$ , and  $\tau_1 = 0.668 \pm 0.065$  ps,  $\tau_2 = 3.34 \pm 0.67$  ps, and  $\tau_3 = 22.1 \pm 0.4$  ps.

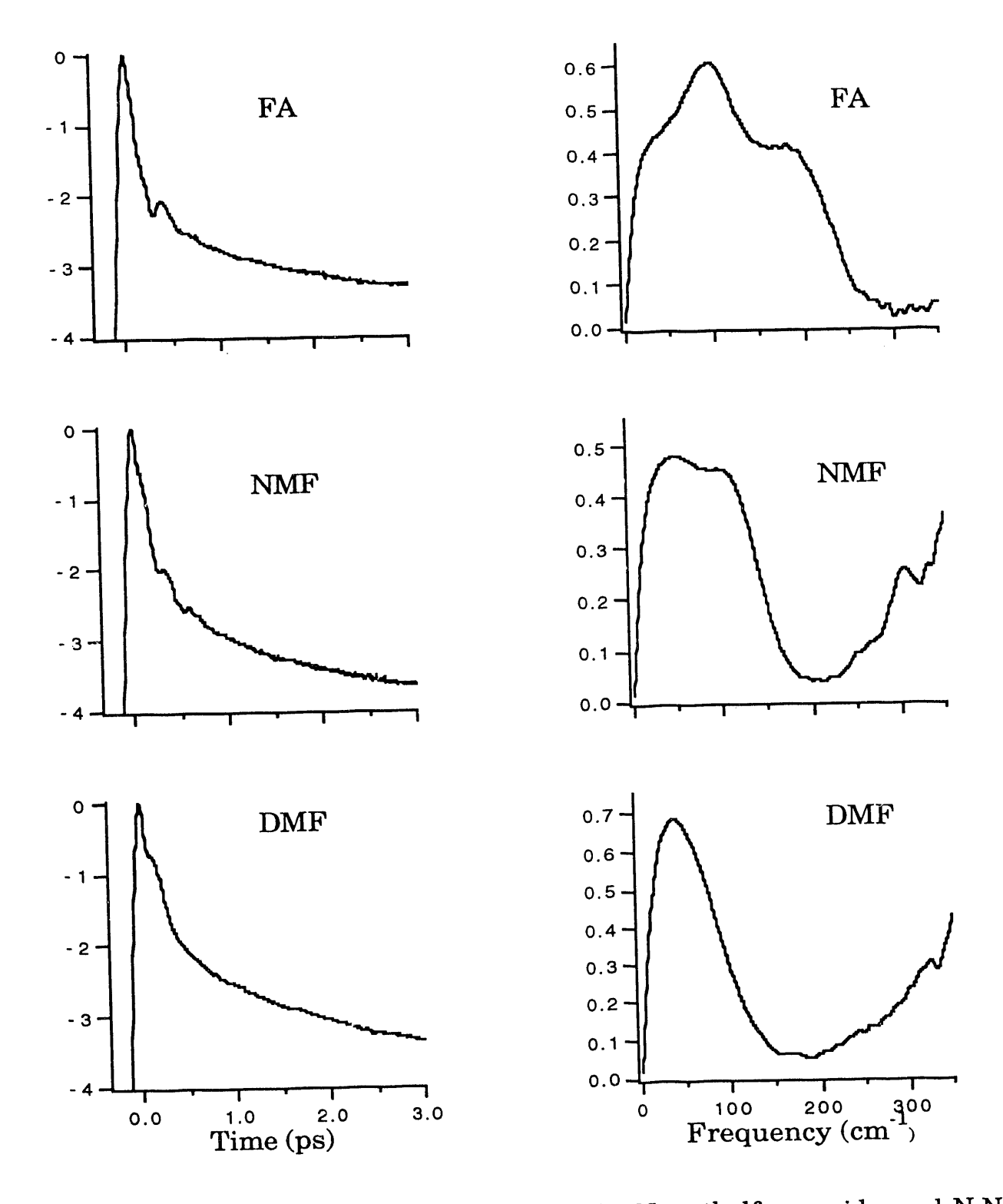


Figure 3. The OHD-RIKES data for formamide, N-methylformamide, and N,N-dimethylformamide are shown. The raw data in the time domain are presented in semi-log form in the left column, with the deconvoluted frequency-domain data obtained from Equations 4 and 5 are shown in the right column with linear ordinate scales.

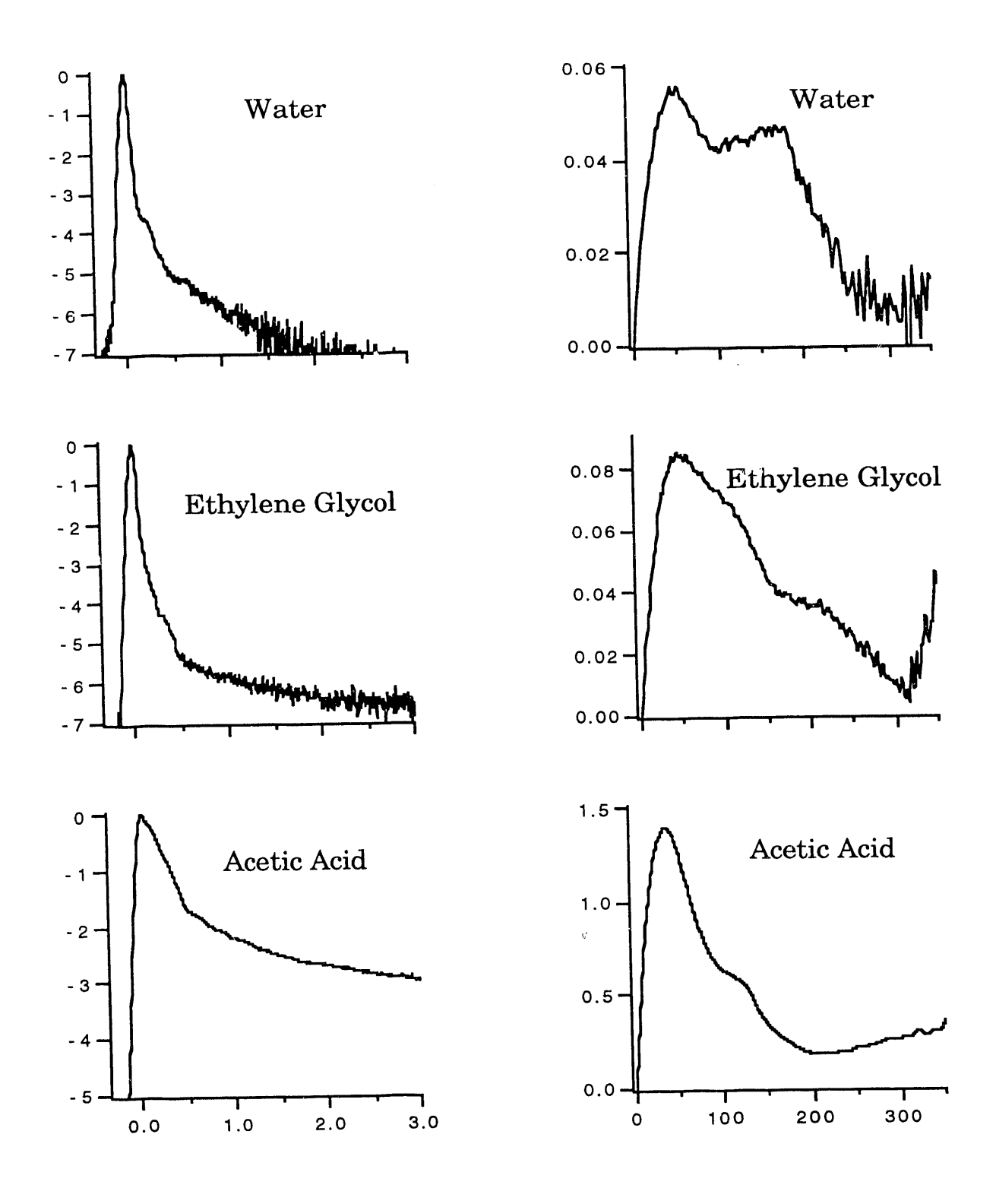


Figure 4. The OHD-RIKES data for water, ethylene glycol, and acetic acid are shown. The raw data in the time domain are presented in semi-log form in the left column, with the deconvoluted frequency-domain data obtained from Equations 4 and 5 are shown in the right column with linear ordinate scales.

of the molecular nonlinear optical response, labeled  $\sigma(t)$  in Equation 1. The signal begins to decay more slowly than the laser pulse autocorrelation starting in the range from 100-300 femtoseconds. This initial rapid decay of the nonlinear optical polarization arises from the nuclear-coordinate inertial motions of the solvent molecules. At time-scales longer than 1.0-1.5 picoseconds, all of the inertial components of the molecular nonlinear optical response are damped out, and only the diffusive rotational reorientation processes contribute to the polarization decay.

For all of the hydrogen-bonding solvents presented here, a rather rapid decay of the birefringence transient occurs after the peak of the signal. Partly this is caused by the very rapid decay of the intermolecular vibrations convoluted with the laser pulse, and partly this is simply a result of the fact that the electronic hyperpolarizability component of the response dominates the overall molecular response, R(t), except for acetic acid. For acetic acid, the diffusive part of the nuclear relaxation dominates, leading to a much slower decay of the OHD-RIKES transient in the first 0.5 ps.

For the formamides, water, and ethylene glycol, a substantial change in curvature occurs in the OHD-RIKES birefringence transients at a time delay between 200-300 femtoseconds. In each of these cases, this "knee" of the curve results from the underdamped intermolecular vibrations: out-of-plane librations for the formamides, (Chang and Castner, 1993) and translational density fluctuations for water (Chang and Castner, 1993).

When the OHD-RIKES femtosecond dynamics are considered in the frequency domain, it is possible to remove the rotational diffusion response exactly in the time domain, prior to deconvolution of the electronic response. This is done by fitting the longer time multi-exponential tails, and subtracting this part using Equation 7. We have done this analysis for all of our data sets, and the results are shown in the right hand columns of Figures 3 and 4. The resulting nuclear-coordinate spectral density then contains only the inertial parts of the solvent relaxation. For all the liquids studied, there is a peak in the low-frequency spectraldensity occurring near 50 cm<sup>-1</sup>. This low-frequency band results from a complex sum of intermolecular interactions including overdamped librations and interaction-induced Raman modes that result from intermolecular collisions. The higher frequency modes with band centers in the 100-250 cm<sup>-1</sup> range have been assigned to librations and translations for acetic acid (Faurskov Nielsen and 1983), formamide (Faurskov-Nielsen, et al., 1982), ethylene glycol (Manisse-Morgant, et al., 1971; Schwartz, 1977), and water (Walrafen, 1990) based on low-frequency Raman studies in the frequency domain.

We analyze our low-frequency spectral density obtained from applying Equations 7, 4, and 5 to our data, in terms of a sum of different classical oscillators. The librational and translational bands are fit to sums of Gaussian or anti-symmetrized Gaussian models. The broadest asymmetric lowest-frequency band has been assigned to collisional interaction-induced effects in simpler liquids, and is often fit to a

function form of the type  $I(\omega) = \omega^{\alpha} \exp(-\omega/\omega_0)$ , where the exponent  $\alpha$  is usually near unity.

Figures 5A and 5B show the solvation time-correlation functions, for an instantaneously-created charge,  $C_V(t)$ , for the three formamides, and acetic acid, ethylene glycol, and water, respectively. These curves were calculated using Equation 8. The initial parts of the decays of  $C_V(t)$  all show a Gaussian shape, indicating the inertial character of this part of the solvation response. For longer times beyond ~250 fs, the Gaussian initial decay trails into a non-exponential response arising from the diffusive rotational reorientation.

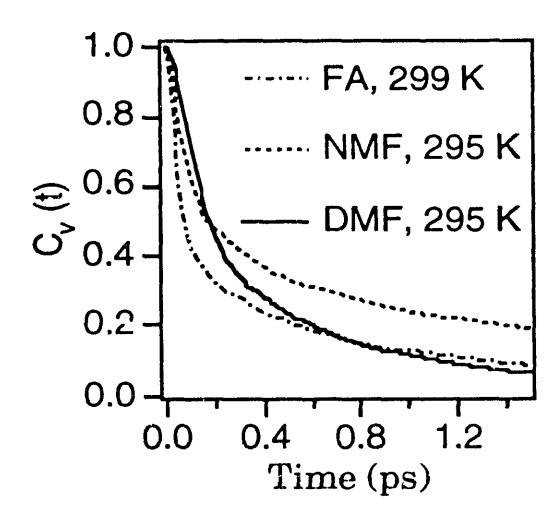


Figure 5A. The solvation correlationfunction for an instantaneously created charge, Cv(t), are shown. Cv(t) is calculated using Equation 3. Formamide, N-methylformamide, and N,Ndimethylformamide.

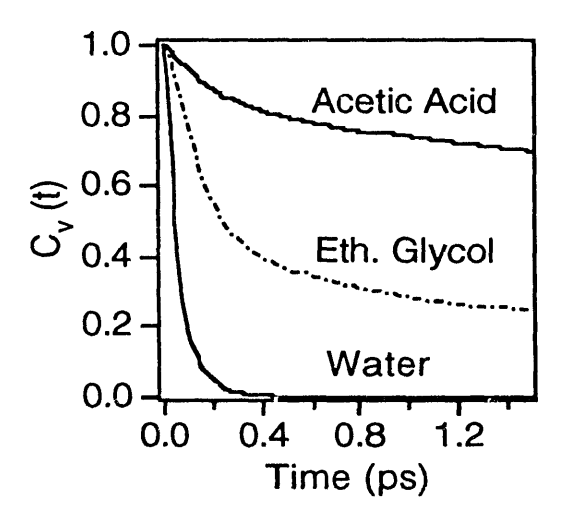


Figure 5B. Cy(t) for acetic acid, ethylene glycol, and water are shown.

For comparison with TDFSS experiments and molecular dynamics simulations, we define an effective integrated solvation time constant  $\tau_S$  as

 $\tau_{\rm S} = \int_0^{\rm C} C_{\rm V}(t) {\rm d}t$ . The effective solvation times,  $\tau_{\rm S}$ , are given in Table 1. Though the effective solvation times for NMF, acetic acid, and ethylene glycol all exceed 1.0 picosecond, Figure 5 clearly shows that extremely rapid inertial processes are present in all of the six hydrogen-bonding solvents that we have measured.

Table 1

Solvent	$ au_{ m S}( m ps)$
formamide	0.46
NMF	1.1
DMF	0.45
acetic acid	15.2
ethylene glycol	1.76
water	0.074

Recent theoretical work has concentrated on understanding the ultrarapid inertial motions in terms of multi-mode Brownian oscillators (Fried and Mukamel, 1993) and using an intermolecular normal vibrational mode analysis (Buchner, et al., 1992). We are presently extending our data analysis to include these newer and more sophisticated models for the inertial dynamics and low-frequency spectra.

### ACKNOWLEDGMENTS

This research was carried out at Brookhaven National Laboratory under contract DE-AC02-76CH00016 with the U.S. Department of Energy and supported by its Division of Chemical Sciences, Office of Basic Energy Sciences.

### REFERENCES

Buchner, M., Ladanyi, B. M. and Stratt, R. M., 1992-The short-time dynamics of molecular liquids. Instantaneous-normal-mode theory. In: J. Chem. Phys., <u>97</u>, 8522-8535

Chang, Y. J. and Castner, E. W., Jr., 1993-Fast Responses From "Slowly-Relaxing" Liquids: A Comparison Between The Femtosecond Dynamics Of Triacetin, Ethylene Glycol, And Water. In: submitted for publication.

Chang, Y. J. and Castner, E. W., Jr., 1993-Femtosecond dynamics in hydrogen-bonding solvents: Formamide and N-methylformamide in acetonitrile, DMF, and water. In: J. Chem. Phys., 99, in press, 01 July

Cho, M., Rosenthal, S. J., Scherer, N. F., Ziegler, L. D. and Fleming, G. R., 1992-Ultrafast solvent dynamics: Connection between time resolved fluorescence and optical Kerr

measurements. In: J. Chem. Phys., **96**, 5033-5038

Duguay, M. A. and Hansen, J. W., 1969-An ultrafast light gate. In: Appl. Phys. Lett., **15**, 192-194

Etchepare, J., Grillon, G., Hamoniaux, G. and Orszag, A., 1987- In: Opt. Commun., 63, 329

Faurskov Nielsen, O. and Lund, P.-A., 1983-Intermolecular Raman active vibrations of hydrogen bonded acetic acid dimers in the liquid state. In: J. Chem. Phys., 78, 652-655

Faurskov-Nielsen, O., Lund, P.-A. and Praestgaard, E., 1982-Hydrogen bonding in liquid formamide. A low frequency Raman study. In: J. Chem. Phys., 77, 3878-3883

Fried, L. E. and Mukamel, S., 1993-Simulation of Nonlinear Electronic Spectroscopy in the Condensed Phase. In: Advances in Chemical Physics, 84, 435-517

Greene, B. I. and Farrow, R. C., 1982-Direct measurement of a subpicosecond birefringent response in CS2. In: J. Chem. Phys., 77, 4779-4780

Hattori, T., Terasaki, A., Kobayashi, T., Wada, T., Yamada, A., et al., 1991-Optical-heterodyne-detected induced phase modulation for the study of femtosecond molecular dynamics. In: J. Chem. Phys., **95**, 937-945

Kohler, B. and Nelson, K. A., 1992-Femtosecond impulsive stimulated light scattering from liquid carbon disulfide at high pressure: Experiment and computer simulation. In: J. Phys. Chem., **96**, 6532-6538

Levenson, M. D. and Eesley, G. L., 1979-Polarization selective optical heterodyne detection for dramatically improved sensitivity in laser spectroscopy. In: Appl. Phys., 19, 1-17

Manisse-Morgant, A., Beaudoin, J. L., Benchenane, A. and Harrand, M., 1971-Contribution à l'étude de la structure de l'éthylèneglycol liquide et cristallisé. In: C. R. Acad. Sci., 273B, 293-296

Maroncelli, M., Kumar, V. P. and Papazyan, A., 1993-A Simple Interpretation of Polar Solvation Dynamics. In: J. Phys. Chem., **97**, 13-18

McMorrow, D., 1991-Separation of nuclear and electronic contributions to femtosecond four-wave mixing data. In: Opt. Commun., <u>86</u>, 236-244

McMorrow, D., Kim, S. K., Melinger, J. S. and Lotshaw, W. T., 1992-Probing the microscopic molecular environment in liquids with femtosecond Fourier-transform Raman spectroscopy. In: Ultrafast Phenomena VIII, in press

McMorrow, D. and Lotshaw, W. T., 1993-Evidence for low-frequency (~15 cm-1) collective modes in benzene and pyridine liquids. In: Chem. Phys. Lett., 201, 369

McMorrow, D. and Lotshaw, W. T., 1991-Intermolecular Dynamics in Acetonitrile Probed with Femtosecond Fourier Transform Raman Spectroscopy. In: J. Phys. Chem., <u>95</u>, 10395-10406

McMorrow, D., Lotshaw, W. T. and Kenney-Wallace, G. A., 1988-Femtosecond Optical Kerr Studies on the Origin of the Nonlinear Responses in Simple Liquids. In: IEEE J. Quantum Electron., 24, 443-454

Ruhman, S., Joly, A. G. and Nelson, K. A., 1988-Coherent Molecular Vibrational Motion Observed in the Time Domain Through Impulsive Stimulated Raman Scattering. In: IEEE J. Quantum Electron., 24, 470-481

Ruhman, S., Kohler, B., Joly, A. G. and Nelson, K. A., 1987-Intermolecular vibrational motion in CS2 liquid at 165  $K \le T \le 300$  K observed by femtosecond time-resolved impulsive stimulated scattering. In: Chem. Phys. Lett., 141, 16-24

Schwartz, M., 1977-Raman study of the conformational equilibrium of ethylene glycol in dimethyl sulfoxide. In: Spectrochim. Acta, <u>33A</u>, 1025-1032

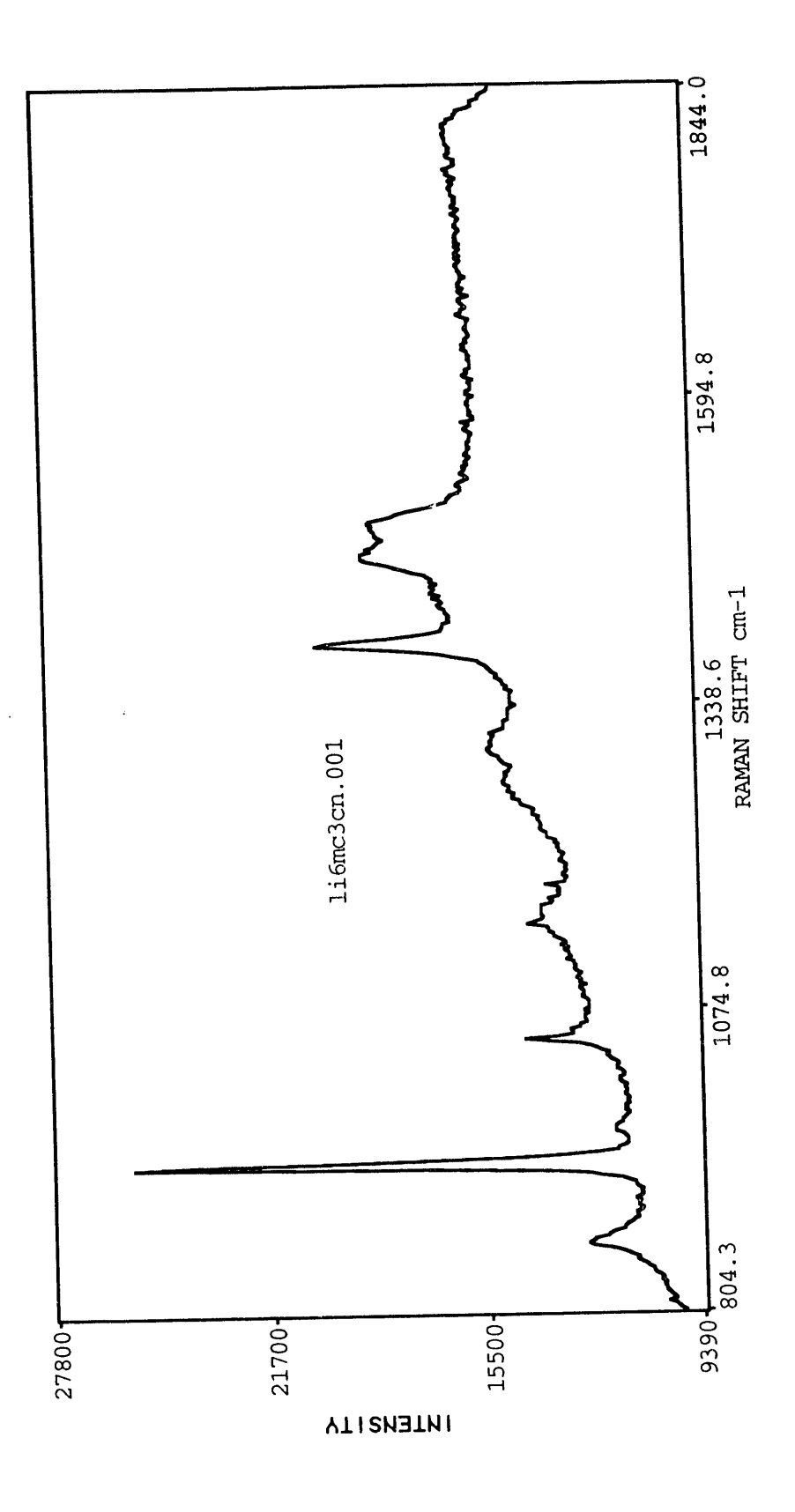
Walrafen, G. E., 1990-Raman Spectrum of Water: Transverse and Longitudinal Acoustic Modes Below ≈300 cm<sup>-1</sup> and Optic Modes Above ≈300 cm<sup>-1</sup>. In: J. Phys. Chem., **94**, 2237-2239

Wynne, K., Galli, C. and Hochstrasser, R. M., 1992-Femtosecond intermolecular vibrational motion in pyrrole. In: Chem. Phys. Lett., 193, 17-22

Yan, Y.-X., Cheng, L.-T. and Nelson, K. A., 1988-Impulsive Stimulated Light Scattering. In: Advances in Nonlinear Spectroscopy, 16, 299-355

### **AUTHORS' ADDRESS**

Brookhaven National Laboratory Chemistry Department Building 555A Upton, NY 11973 U.S.A.



li6mc3cn.001 Created 06/21/93 at12h4lm36s; ET=400s; Exps= 1 LiCF3SO3/MC3/CH3CN 1/6/1G 6-21-93

# DATE FILMED 11/5/93

